PCCP

Accepted Manuscript

ROYAL SOCIETY OF CHEMISTRY

www.rsc.org/pccp

Journal Name

ARTICLE

Probing the Early Stages of Solvation of *cis*-Pinate Dianion by Water, Acetonitrile, and Methanol: A Photoelectron Spectroscopy and Theoretical Study†

Received 00th January 20xx,
Accepted 00th January 20xx

DOI: 10.1039/x0xx00000x

www.rsc.org/

Gao-Lei Hou,‡[a] Xiang-Tao Kong,‡[b] Marat Valiev,[a] Ling Jiang,*[b] and Xue-Bin Wang*[a]

Cis-pinic acid is one of the most important oxidation products of α-pinene – a key monoterpene compound in biogenic emission processes. Molecular level understanding of its interaction with water in cluster formation is an important and necessary prerequisite toward ascertaining its role in the aerosol formation processes. In this work, we studied the structures and energetics of the solvated clusters of *cis*-pinate (*cis*-PA^{2-}), the doubly deprotonated dicarboxylate of *cis*-pinic acid, with H_2O, CH_3OH, and CH_3CN by negative ion photoelectron spectroscopy and *ab initio* theoretical calculations. We found that *cis*-PA^{2-} prefers being solvated alternately on the two $-CO_2^-$ groups with increase of solvent coverage, a well-known solvation pattern that has been observed in microhydrated linear dicarboxylate dianion (DC_n^{2-}) clusters. Experiments and calculations further reveal an intriguing feature for the existence of the asymmetric type isomers for *cis*-$PA^{2-}(H_2O)_2$ and *cis*-$PA^{2-}(CH_3OH)_2$, in which both solvent molecules interact with only one of the $-CO_2^-$ groups – a phenomena that has not been observed in DC_n^{2-} water clusters and exhibits the subtle effect of the rigid four-membered carbon ring brought in on the *cis*-PA^{2-} solvation. The dominant interactions between *cis*-PA^{2-} and solvent molecules form bidentate $O^-\cdots H-O$ H-bonds for H_2O, $O^-\cdots H-O$ and $O^-\cdots H-C$ H-bonds for CH_3OH, and tridentate $O^-\cdots H-C$ H-bonds for CH_3CN. The formation of inter-solvent H-bonds between H_2O and CH_3CN is found to be favorable in mixed solvent clusters, different from that between H_2O and CH_3OH. These findings have important implications for understanding the mechanism of cluster growth and formation of atmospheric organic aerosols, as well as for rationalizing the nature of structure-function relationship of proteins containing carboxylate groups under various solvent environments.

Introduction

Cis-pinic acid (*cis*-PA), a C_9-dicarboxylic acid with a rigid, four-membered carbon ring linking two inequivalent carboxylic groups (α and β; Scheme 1), is one of several distinct oxidation products of α-pinene,[1-7] which is the most abundant emission from natural plants.[5,8] With the upper limits of the partial vapor pressure of $(5.6\pm4.0)\times10^{-8}$ Torr,[3] *cis*-PA can be classified as a semivolatile organic compound (SVOC),[7, 9] and is found to play an important role in the formation of new aerosol particles.[2-4, 10] The contributions of those organic aerosol particles to the global aerosol budget have very complicated mechanisms with high uncertainties.[10-19] Such complexity and uncertainty hamper the quantitative elucidation of their effects on the Earth's radiation balance.[20-22]

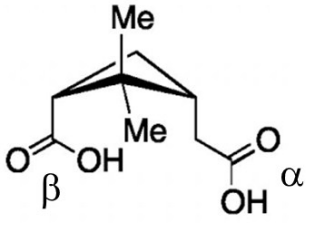

Scheme 1. *Cis*-pinic acid

With two carboxylic groups, *cis*-PA has the potential to form clusters with itself and other precursors like H_2O molecules.[11, 18, 23, 24] In the atmospheric environment, humidity is always one of the key parameters to drive the final stage of new particles growth and thus it would be important to investigate the fate of *cis*-PA in humid environments,[25] i.e., the interaction of *cis*-PA with H_2O.

On the other hand, as a deprotonated conjugate base of a dicarboxylic acid, *cis*-pinate (*cis*-PA^{2-}) is also important in biochemistry[26] and synthetic chemistry,[27] and can be viewed

[a] *Pacific Northwest National Laboratory, 902 Battelle Boulevard, P. O. Box 999, MS K8-88, Richland, Washington 99352, USA.* Email: xuebin.wang@pnnl.gov
[b] *State Key Laboratory of Molecular Reaction Dynamics, Collaborative Innovation Center of Chemistry for Energy and Materials, Dalian Institute of Chemical Physics, Chinese Academy of Sciences, 457 Zhongshan Road, Dalian 116023, Liaoning, P. R. China.*
Email: ljiang@dicp.ac.cn

†Electronic Supplementary Information (ESI) available: The 20 K photoelectron spectrum of bare *cis*-PA^{2-} at 266 nm (Fig. S1); Comparison of experimental VDE value to calculated ones for the bare *cis*-PA^{2-} dianion at different theoretical levels (Table S1); Comparison of experimental VDEs to calculated ones and the relative energies (ΔE) of different isomers for the solvated *cis*-PA^{2-} clusters at different theoretical levels (Table S2); Cartesian coordinates and energies for all isomers. See DOI: 10.1039/x0xx00000x

‡These authors contributed equally to this work.

as a simple model for peptide chains in slightly basic solutions. Thus a molecular understanding of its interactions with different solvents such as H_2O, CH_3CN, and CH_3OH will be helpful to address the protein functions and structures in various solvent environments.[28-32]

In this work, we carried out a joint negative ion photoelectron spectroscopy (NIPES) and *ab initio* theoretical calculations on a series of size-selective *cis*-PA^{2-} solvated clusters to examine the early stages of the *cis*-PA^{2-} solvation with H_2O, CH_3CN, and CH_3OH. Unlike those dicarboxylates with linear and flexible aliphatic chains ($^-O_2C(CH_2)_nCO_2^-$, DC_n^{2-}, n = 2-12) previously studied,[33-38] *cis*-PA^{2-} contains a rigid, four-membered carbon ring with two inequivalent carboxylate groups (Scheme 1). Overall, we found that *cis*-PA^{2-} shows a similar solvation pattern compared to those of DC_n^{2-} interacting with water molecules, but subtle differences are unraveled. Meanwhile, we have systematically investigated *cis*-PA^{2-} solvation with CH_3CN and CH_3OH, two common nonaqueous solvents.[32, 39, 40] This represents the first NIPES study of carboxylate solvation beyond solvent water, and reveals interesting and distinctly different solvation motifs that may help understanding protein functions and structures under various solvent environments.

Experimental Methods

The NIPES experiments were performed using a low-temperature, magnetic-bottle time-of-flight (TOF) photoelectron spectrometer, coupled with an electrospray ionization source and a temperature-controllable cryogenic ion-trap.[41] The *cis*-pinate-solvent cluster dianions (*cis*-$PA^{2-}(Sol)_m(H_2O)_n$; Sol = CH_3CN and CH_3OH) were produced via electrospraying into the gas phase from a 0.1 mM solution of *cis*-pinic acid, dissolved in water/acetonitrile or methanol, with the solution pH value tuned to around 8 by adding ~100 mM aqueous NaOH solution dropwise. The produced ions were accumulated and collisionally cooled in the cryogenic 3D ion trap set at 20 K for 20-100 ms, minimizing the populations of high energy isomers and eliminating the extra features due to vibrational hot bands in the photoelectron spectra. The cold ions were then transferred into the extraction zone of a TOF mass spectrometer for mass and charge analyses.

During each NIPES experiment, the desired *cis*-$PA^{2-}(Sol)_m(H_2O)_n$ dianions were mass-selected and decelerated before being photodetached by a ArF laser beam (193 nm, 6.424 eV). The laser was operated at a 20 Hz repetition rate with the ion beam off at alternating laser shots to enable shot-by-shot background subtraction. Photoelectrons were collected at nearly 100% efficiency by the magnetic-bottle and analyzed in a 5.2 m long electron flight tube. The TOF photoelectron spectra were converted into electron kinetic energy spectra by calibration with the known NIPE spectra of I^- and $OsCl_6^{2-}$. The electron binding energies (EBEs), given in the spectra in Figs. 1-3 were obtained by subtracting the electron kinetic energies from the detachment photon energy. The experimental vertical detachment energy (VDE) of each cluster anion was measured from the maximum of the first resolved peak in the respective NIPE spectrum.

Theoretical Details

Quantum chemical calculations were performed using Gaussian 09 program suite.[42] Several methods, i.e. M06-2X, ωB97X-D, B3LYP, BHLYP, BLYP, BP86, PBE, PW91, TPSS, and MP2 have been tested for the bare *cis*-PA^{2-} dianion (See Table S1 in the ESI), showing that M06-2X/aug-cc-pVDZ and ωB97X-D/aug-cc-pVDZ yield better results than others. Furthermore, recent investigations have demonstrated that M06-2X hybrid functional can well reproduce the photoelectron spectroscopic experiments of solvated carboxylate anions.[24, 43] Therefore, this functional was employed for the present calculations as well. The aug-cc-pVDZ basis set was used for all atoms. Structures were optimized using tight convergence criteria without any symmetry restrictions. Harmonic vibrational frequency analyses were carried out to confirm that the structures were real minima. Theoretical VDEs were calculated as the total energy differences between the dianions and the one-electron less monoanions both at the optimized geometries of the dianions. Relative energies obtained from the M06-2X/aug-cc-pVDZ optimization were almost the same as those from MP2/aug-cc-pVDZ//M06-2X/aug-cc-pVDZ single point energy calculation (Table S2). Therefore, we will focus on the results obtained with M06-2X/aug-cc-pVDZ in the following parts.

Results and Discussions

Photoelectron Spectroscopy

NIPE spectra of *cis*-$PA^{2-}(H_2O)_n$ (n = 0–4)

Fig. 1 shows the 20 K 193 nm NIPE spectra of *cis*-$PA^{2-}(H_2O)_n$ (n = 0–4). Characteristic carboxylate $-CO_2^-X$ and A bands[44] are seen in both the 266 (Fig. S1 in the ESI) and 193 nm spectra for the bare *cis*-PA^{2-}. These bands arise from removal of one electron from the highest occupied molecular orbital (HOMO) (mainly a σ* in-plane antibonding orbital) and from the HOMO-1 orbital (σ in-plane bonding combination) for the X doublet feature, and by detaching one electron from HOMO-2 orbital with an out-of-plane antibonding p character for the A band, respectively.[45-47] The weak broad band denoted with "*" centered at EBE~3.0 eV is a spectral feature due to detachment of the singly charged product monoanion or fragment anion by a second photon, as has been reported in previous studies.[35, 36, 44, 48] A strong signal with near 0 eV kinetic energy electrons is seen near the photon energy limit in the spectrum of *cis*-PA^{2-}. As suggested before,[44, 49] these zero kinetic energy photoelectrons are due to dissociative secondary autodetachment for the primary photodetached product of *cis*-$PA^{\bullet-}$ radical monoanions, which are expected to be highly unstable toward electron autodetachment and loss of CO_2 (decarboxylation).

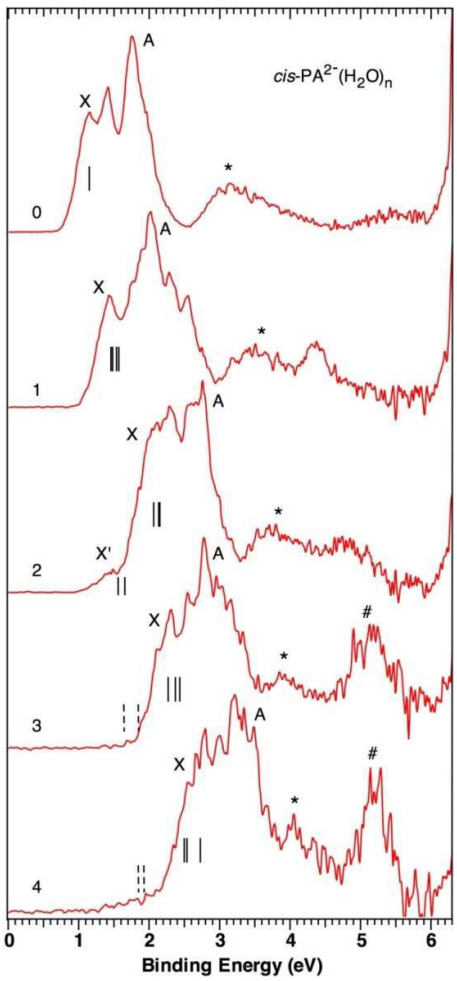

Fig. 1. The 20 K photoelectron spectra of *cis*-$PA^{2-}(H_2O)_n$ (n = 0-4) at 193 nm. The solid and dashed vertical bars are the calculated VDEs from lowest energy isomers (more symmetrically solvated ones aligning with band X) that are likely present in the experiments, and those high energy isomers (highly asymmetrically solvated) that are likely absent in the experiments, respectively.

The NIPE spectra of the solvated clusters *cis*-$PA^{2-}(H_2O)_n$ in Fig. 1 show overall similar spectral pattern compared to the bare solute with incremental increase of EBE per water molecule (Table 1). Close examination of the spectra reveals interesting odd-even variations with the number of solvent water for both EBE and spectral band shape. Upon solvation by one H_2O, the spectrum of *cis*-$PA^{2-}(H_2O)_1$ shifts to high binding energy by 0.3 eV and becomes appreciably (by 30%) broader. This is because, when there is only one water molecule, either α or β carboxylate group is solvated, resulting in two more inequivalent carboxylate ends, one $-CO_2^-$, and the other $-CO_2^-(H_2O)_1$. The VDE of *cis*-$PA^{2-}(H_2O)_1$ is measured from the $-CO_2^-$ end, which is only indirectly affected by the water at the other end of *cis*-PA^{2-}. The contributions of these two

Table 1. The experimentally measured vertical detachment energies (VDEs) of *cis*-$PA^{2-}(Sol)_m(H_2O)_n$ clusters.

Clusters	VDE (eV)	
	X	X′
cis-PA^{2-}	1.15± 0.05	
cis-$PA^{2-}(H_2O)$	1.43 ± 0.05	
cis-$PA^{2-}(CH_3CN)$	1.44 ± 0.05	
cis-$PA^{2-}(CH_3OH)$	1.44 ± 0.05	
cis-$PA^{2-}(H_2O)_2$	2.07± 0.10	1.45 ± 0.05
cis-$PA^{2-}(CH_3CN)_2$	2.08 ± 0.05	
cis-$PA^{2-}(CH_3OH)_2$	2.10± 0.10	1.60± 0.10
cis-$PA^{2-}(H_2O)_3$	2.30 ± 0.05	
cis-$PA^{2-}(H_2O)_4$	2.75 ± 0.10	
cis-$PA^{2-}(CH_3CN)(H_2O)$	2.07 ± 0.05	1.50 ± 0.10
cis-$PA^{2-}(CH_3OH)(H_2O)$	2.08 ± 0.05	
cis-$PA^{2-}(CH_3CN)(H_2O)_2$	2.29 ± 0.05	1.60 ± 0.10

inequivalent carboxylate ends with different EBEs also significantly broaden the overall spectral bandwidth. When the second solvated H_2O adds, the VDE of cis-$PA^{2-}(H_2O)_2$ is increased by 0.6 eV, and the spectral band becomes narrower relative to that at n = 1. This observation strongly suggests that the second water solvates the un-solvated $-CO_2^-$ in the n = 1 cluster, resulting in two carboxylate ends both being solvated by one H_2O, which reduces the chemical discrepancy of these two carboxylate ends and consequently narrows the spectral band. The VDE increase of n = 2 from n = 1, i.e., ΔVDE (1→2, ~0.6 eV), reflects a direct solvation effect on the negative charge instead of an indirect charge-dipole stabilization for ΔVDE (0→1, ~0.3 eV), and is expected to be larger. This odd-even effect seems recurring to n = 3 and 4, indicating an alternating solvation pattern for *cis*-PA^{2-}, similar to the solvation pattern observed for the aliphatic dicarboxylate DC_n^{2-} dianions.[33-38] The above inference on solvation evolution reached from the analyses of the VDEs and spectral bands is also born out from our theoretical calculations (vide infra). It is notable that there is an additional weak X′ band with low EBE = 1.45 eV in the n = 2 spectrum, suggesting coexistence of multiple isomers for this cluster. Besides the X, A, and "*" bands, a high EBE spectral band "#", which is obvious in n = 3 and 4 and discernible in n = 1 and 2, is observed. The intensity of this band increases with water molecules. The nature of this band, as suggested before, is due to the ionization of solvent water molecules,[35, 36, 50] whose ionization potential is significantly lowered by the presence of multiply charged negative ions in vicinity. The VDEs of *cis*-PA^{2-} and its solvated clusters *cis*-$PA^{2-}(H_2O)_n$ measured from the maxima (centers) of the first resolved bands are summarized in Table 1.

NIPE spectra of *cis*-$PA^{2-}(Sol)_m$ (Sol = CH_3CN and CH_3OH, m = 1 and 2)

The NIPE spectra of *cis*-$PA^{2-}(CH_3CN)_m$ in Fig. 2 show a very similar trend in EBE and spectral bandwidth with the increase of the solvent molecules as that in *cis*-$PA^{2-}(H_2O)_n$. The stepwise

increase of EBE per CH_3CN, i.e. 0.3 and 0.6 eV for the first and second acetonitrile molecule, respectively, is identical within

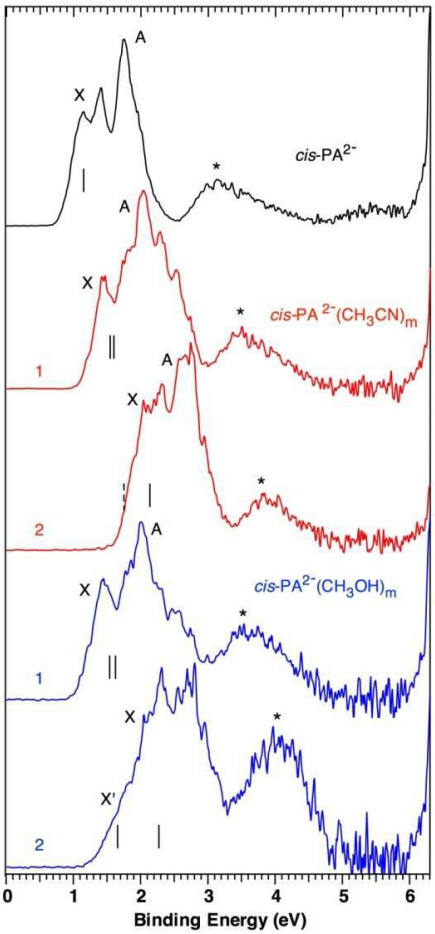

Fig. 2. The 20 K photoelectron spectra of *cis*-$PA^{2-}(Sol)_m$ (Sol = CH_3CN and CH_3OH; m = 1 and 2) at 193 nm. The solid and dashed vertical bars are the calculated VDEs from lowest energy isomers (more symmetrically solvated ones aligning with band X) that are likely present in the experiments, and those high energy isomers (highly asymmetrically solvated) that are likely absent in the experiments, respectively.

experimental uncertainties to what is observed in the water case (Table 1); the spectral band for m = 1 is significantly broader than that for m = 0 and 2. These spectral revelations suggest a similar alternating solvation on the two $–CO_2^-$ ends of *cis*-PA^{2-} in CH_3CN as in H_2O.

Upon solvation by one CH_3OH, the spectrum of *cis*-$PA^{2-}(CH_3OH)$ shifts to higher EBE, again by ~0.3 eV (EBE = 1.44 eV, Table 1) relative to that of bare *cis*-PA^{2-}; the spectral band is also similar to the clusters with one H_2O or one CH_3CN discussed above. While the EBE for the main spectral band in *cis*-$PA^{2-}(CH_3OH)_2$ is ~2.10 eV, similar to that with two H_2O or CH_3CN molecules, there exists a notable feature at EBE~1.60 eV, with which the EBE is only slightly larger than that of *cis*-$PA^{2-}(CH_3OH)$. This seems to suggest that besides the symmetric solvation with one CH_3OH on each $–CO_2^-$ end, asymmetric solvation isomers with both CH_3OH molecules

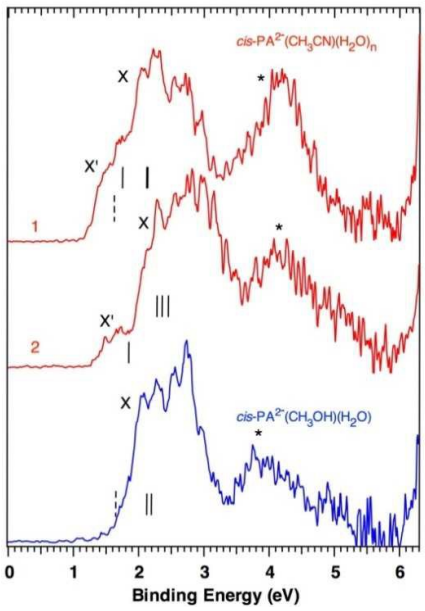

Fig. 3. The 20 K photoelectron spectra of *cis*-$PA^{2-}(Sol)(H_2O)_n$ (Sol = CH_3CN and CH_3OH; n = 1 and 2) at 193 nm. The solid and dashed vertical bars are the calculated VDEs from lowest energy isomers (more symmetrically solvated ones aligning with band X) that are likely present in the experiments, and those high energy isomers (highly asymmetrically solvated) that are likely absent in the experiments, respectively.

solvating one $–CO_2^-$ end may exist to give rise to this low EBE feature. Our theoretical calculations described below fully support the above predictions on *cis*-$PA^{2-}(CH_3CN/CH_3OH)_m$ solvation.

NIPE spectra of *cis*-$PA^{2-}(Sol)(H_2O)_n$ (Sol = CH_3CN and CH_3OH, n = 1 and 2)

Fig. 3 shows the NIPE spectra of the mixed solvent clusters. The spectrum of *cis*-$PA^{2-}(CH_3CN)(H_2O)$ is notably broader than those of *cis*-$PA^{2-}(CH_3CN)_2$ and *cis*-$PA^{2-}(H_2O)_2$, in which besides a main spectral band with EBE~2.10 eV, a low binding energy feature with significant intensity is shown at EBE~1.50 eV. The presence of this low binding energy feature in the spectrum of *cis*-$PA^{2-}(CH_3CN)(H_2O)$ indicates that an isomer with both CH_3CN and H_2O solvating the same $–CO_2^-$ group in *cis*-$PA^{2-}(CH_3CN)(H_2O)$ is among the lowest energy structures that are accessible under the experimental conditions. For *cis*-$PA^{2-}(CH_3CN)(H_2O)_2$, besides the main band feature with EBE = 2.30 eV, it is unexpected to see a weak band with EBE~1.60 eV, a value that is low enough that has to be derived from detaching a "naked" $–CO_2^-$ group. This observation suggests that a highly asymmetric solvation structure with all the solvent (two water and one acetonitrile) molecules solvating only one $–CO_2^-$ group in *cis*-PA^{2-} is also populated.

The main spectral band of *cis*-$PA^{2-}(CH_3OH)(H_2O)$ is similar to that in *cis*-$PA^{2-}(H_2O)_2$ as expected; but considerably simpler than that of *cis*-$PA^{2-}(CH_3CN)(H_2O)$. Thus, the substitution of

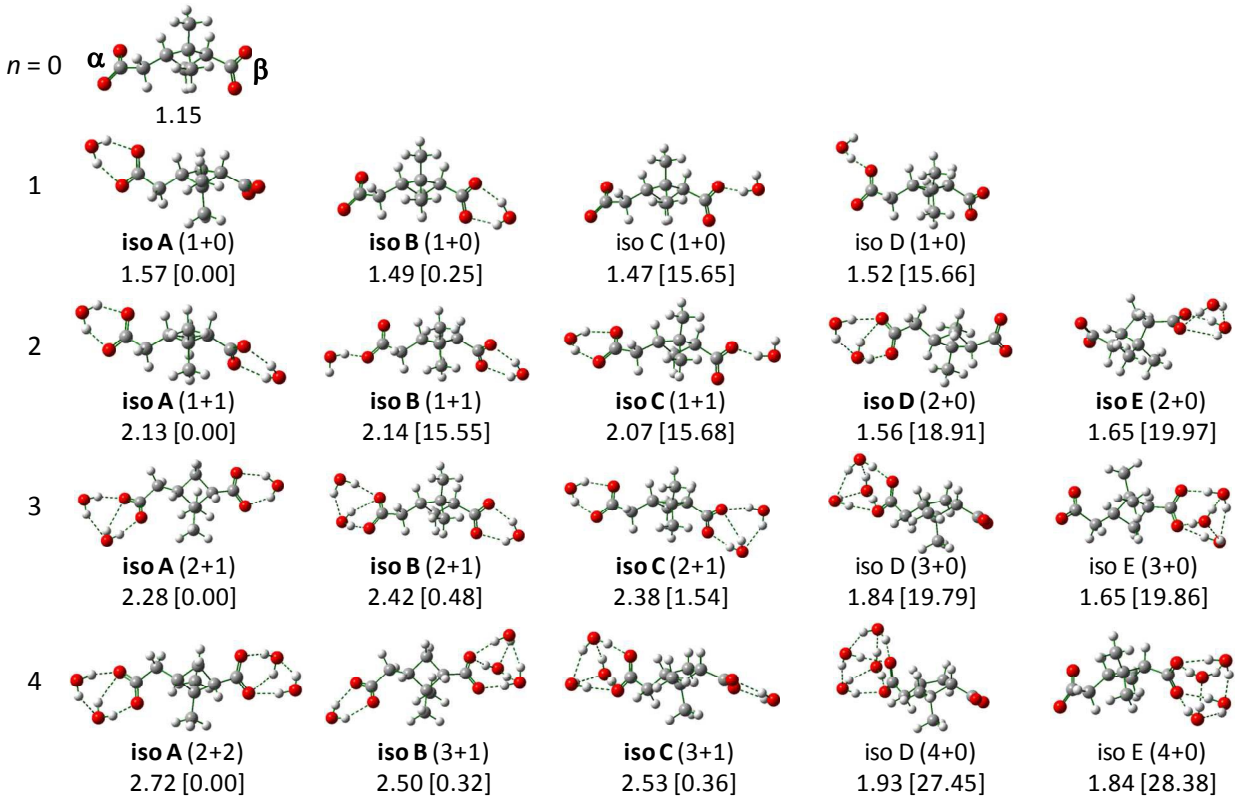

Fig. 4. M06-2X/aug-cc-pVDZ optimized structures of *cis*-PA^{2-} and *cis*-$PA^{2-}(H_2O)_n$ clusters (n = 0-4 as indicated in the first column) (O, red; C, gray; H, light gray). The calculated VDEs (in eV) and relative energies (ΔE in kJ/mol, inside square brackets) are given. The isomers in bold are the ones most likely exist in the experiments.

CH_3CN in *cis*-$PA^{2-}(CH_3CN)(H_2O)$ by CH_3OH in *cis*-$PA^{2-}(CH_3OH)(H_2O)$ results in distinct differences in the formation of H-bonding between CH_3CN and $-CO_2^-$ group compared to that between CH_3OH/H_2O and $-CO_2^-$ group. As it will become clear from our theoretical calculations described below, one CH_3CN can form a triple H-bond via three H atoms in its methyl group with two oxygen atoms in $-CO_2^-$ end, in contrast to solvent H_2O and CH_3OH, which mainly interact with the carboxylate oxygen atoms via forming bidentate $O^-\cdots H-O$ H-bonds for H_2O, and $O^-\cdots H-O$ and $O^-\cdots H-C$ H-bonds for CH_3OH.

Optimized Structures

Considering that the solvent molecule forms H-bond either with the α or β side $-CO_2^-$ group, each structure is labelled with (*x*+*y*), where the values of *x* and *y* indicate the extent of solvation of each $-CO_2^-$ group. This alternative classification scheme will be helpful to compare solvation pattern in the complexes containing more than one solvent molecule. For instance, iso A for *cis*-$PA^{2-}(H_2O)_2$ in Fig. 4 is labelled as (1+1), and iso D as (2+0).

***cis*-$PA^{2-}(H_2O)_n$ (*n* = 1-4)**

Fig. 4 shows the optimized structures of the low energy isomers for *cis*-$PA^{2-}(H_2O)_n$ clusters. In the lowest energy isomer for the monohydrated cluster, the water molecule forms a bidentate H-bond with the α side $-CO_2^-$ (iso A). An alternative bidentate solvation on the β side $-CO_2^-$ gives rise to isomer B, which lies only 0.25 kJ/mol higher in energy. Isomers C and D, each consisting of a singly H-bonded water molecule that interacts with either the β or α $-CO_2^-$, respectively, are calculated to be degenerate in energy by 15.65 and 15.66 kJ/mol higher than isomer A. The calculated VDE values for isomers A–D are 1.57, 1.49, 1.47, and 1.52 eV, respectively (Table 2), which all agree well with the experimental value of 1.43 eV. Since the two lowest-lying isomers A and B are almost energetically identical, both of which should contribute to the experiments, indicating that there is essentially no preference of solvation at the α or β binding site. This holds true for the acetonitrile and methanol molecules as well (*vide infra*). The possible involvement of isomers C and D cannot be excluded, which is reminiscent of a recent infrared photodissociation spectroscopy and *ab initio* molecular dynamics simulation on $H_2PO_4^-(H_2O)$,[51] in which large amplitude motions over a small

barrier, involving the structures with the doubly H-bonded water and the singly H-bonded water were reported. The

Table 2. Comparison of experimental VDE values to calculated ones and relative energies (ΔE) of the isomers for *cis*-$PA^{2-}(H_2O)_n$ (n = 1-4) at the M06-2X/aug-cc-pVDZ level. The isomers in bold are the ones most likely exist in the experiments.

Clusters	Isomers	ΔE (kJ/mol)	VDE (eV)	
			Calc.	Exp.
cis-$PA^{2-}(H_2O)$	**iso A**	0.00	1.57	1.43± 0.05
	iso B	0.25	1.49	
	iso C	15.65	1.47	
	iso D	15.66	1.52	
cis-$PA^{2-}(H_2O)_2$	**iso A**	0.00	2.13	2.07 ± 0.10
	iso B	15.55	2.14	
	iso C	15.68	2.07	
	iso D	18.91	1.56	1.45 ± 0.05
	iso E	19.97	1.65	
cis-$PA^{2-}(H_2O)_3$	**iso A**	0.00	2.28	2.30 ± 0.05
	iso B	0.48	2.42	
	iso C	1.54	2.38	
	iso D	19.79	1.84	
	iso E	19.86	1.65	
cis-$PA^{2-}(H_2O)_4$	**iso A**	0.00	2.72	2.75 ± 0.10
	iso B	0.32	2.50	
	iso C	0.36	2.53	
	iso D	27.45	1.93	
	iso E	28.38	1.84	

energetics for the isomerization will be detailed in the Discussion section.

In the lowest energy isomer of *cis*-$PA^{2-}(H_2O)_2$ (iso A), two water molecules are found to evenly distribute at the α and β sites (1+1), each forming a bidentate H-bond with the respective $-CO_2^-$ group (Fig. 4). Next energetically low-lying isomers B and C (+15.55 and +15.68 kJ/mol) feature one bidentate and one singly H-bonded water molecules interacting with β/α and α/β $-CO_2^-$, respectively. For isomers D and E, which are calculated to lie 18.91 and 19.97 kJ/mol above isomer A, each features two water molecules that form inter-water H-bond and simultaneously solvate only one $-CO_2^-$ end (2+0). The calculated VDE of isomer A (2.13 eV) agrees excellently with the experimental VDE = 2.07 eV determined from the main peak (Table 2). Similar to the monohydrated case, isomers B and C, which feature one singly H-bonded water on one $-CO_2^-$ and one bidentate H-bonded water on the other $-CO_2^-$ end, may also contribute to the main spectral band; and their calculated VDEs are in good accordance with the experimental value. In addition, isomers D and E with the (2+0) solvation configuration, are calculated to have VDEs of 1.56 and 1.65 eV, in agreement with the VDE of the minor peak X′ (1.45 eV) (Fig. 1 and Table 1). Thus they are proposed to exist in the experiments as well and account for the X′ band. This indicates that the inter-water H-bond starts to be present even at n = 2.

For *cis*-$PA^{2-}(H_2O)_3$, isomers A-C are almost energetically identical, in which two waters solvate one $-CO_2^-$ moiety and one water solvates the other $-CO_2^-$ end (2+1). In isomers D and E, three waters make concerted efforts to solvate one $-CO_2^-$ either at the α or β site leaving the other $-CO_2^-$ "naked" (3+0), which are 19.79 and 19.86 kJ/mol above the lowest energy isomer A. The VDEs of isomers A-C are calculated to be 2.28, 2.42, and 2.38 eV, respectively, which are all in good agreement with the experimental value of 2.30 eV (Table 2). Therefore they are proposed to exist in the experiments and contribute to the observed spectrum, Isomers D and E, on the other hand, can be ruled out, because their calculated VDEs are 0.5 and 0.7 eV lower than the experimental VDE, and there is no appreciable low binding energy band observed in the spectrum.

For *cis*-$PA^{2-}(H_2O)_4$, the structure with each $-CO_2^-$ group solvated by two waters is calculated to be the lowest energy isomer (iso A, 2+2). The next lowest energy isomers B and C, in which three waters solvate one $-CO_2^-$ end and one water solvates the other $-CO_2^-$ end (3+1), are found surprisingly favorable, almost degenerate with isomer A (only 0.32 and 0.36 kJ/mol higher in energy). The calculated VDE of isomer A (2.72 eV) agrees best with the experiment (2.75 eV) (Table 2), while the calculated VDEs of isomers B and C (2.50, 2.53 eV) align reasonably to the rising portion of the spectrum (Fig. 1). Therefore we propose that isomers A, B, and C all contribute to the experimental spectrum. The most asymmetric isomers, D and E, in which all of four waters form a H-bonded cage and solvate just one $-CO_2^-$ end (4+0), can be excluded under experimental conditions, because they are higher energy isomers (+27.45 and +28.38 kJ/mol, respectively) and their calculated VDEs are significantly smaller than the experimental value.

cis-$PA^{2-}(CH_3CN)_m$ and *cis*-$PA^{2-}(CH_3OH)_m$ (m = 1 and 2)

For the *cis*-$PA^{2-}(CH_3CN)$ cluster, the acetonitrile molecule is found to solvate one $-CO_2^-$ either at the α site (iso A) or β site (iso B) via forming three H-bonds in-between methyl hydrogen atoms and the negatively charged $-CO_2^-$ group (Fig. 5), a distinctly different solvation motif compared to the water-carboxylate interaction. These two isomers are close in energy as expected. The calculated VDE values of isomer A (1.60 eV) and B (1.53 eV) are consistent with the experimental value of 1.44 eV (Table 3).

The lowest energy isomer of *cis*-$PA^{2-}(CH_3CN)_2$ (iso A) features a symmetric solvation, i.e., each $-CO_2^-$ is solvated by one triply H-bonded acetonitrile (Fig. 5). When both acetonitriles solvate only one $-CO_2^-$ end (for instance, the β site, labeled iso B), the energy of this structure is significantly higher by 22.40 kJ/mol above isomer A. The VDE of isomer A reproduces the experimental value very well (Table 3), while the VDE calculated from the high energy isomer B is appreciably smaller than the experimental value. Hence, we suggest that isomer A is present in the experiments, but not for isomer B.

The overall solvation pattern of *cis*-$PA^{2-}(CH_3OH)_m$ is very similar to that of *cis*-$PA^{2-}(CH_3CN)_m$ depicted above. For the

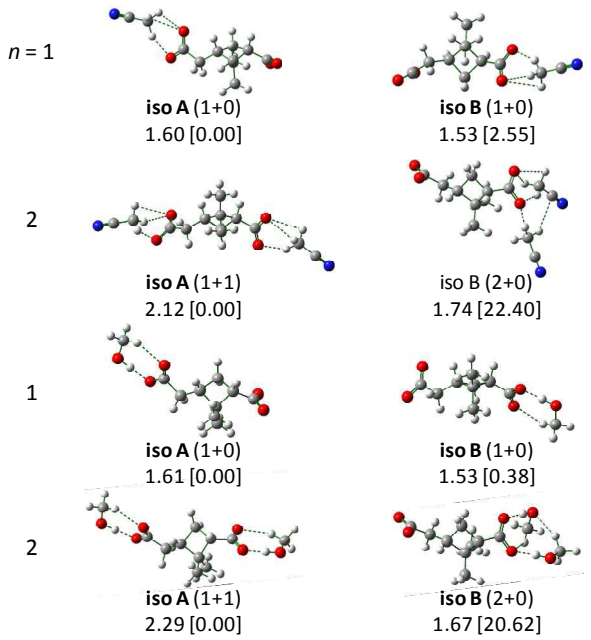

Fig. 5. M06-2X/aug-cc-pVDZ optimized structures of *cis*-$PA^{2-}(CH_3CN)_m$ and *cis*-$PA^{2-}(CH_3OH)_m$ clusters (m = 1, 2 as indicated in the first column) (O, red; C, gray; H, light gray). The calculated VDEs (in eV) and relative energies (ΔE in kJ/mol, inside square brackets) are given. The isomers in bold are the ones most likely exist in the experiments.

mono-solvated *cis*-$PA^{2-}(CH_3OH)$ cluster, the optimized structures with the methanol molecule bound at the α (iso A) or β site (iso B) are energetically identical, which are stabilized by two H-bonds in-between the negatively charged $-CO_2^-$ moiety with one methyl hydrogen atom ($O^-\cdots H-C$) and one hydroxyl hydrogen atom ($O^-\cdots H-O$) (Fig. 5). Optimization of the initial structure with three methyl hydrogen atoms coordinated to the $-CO_2^-$ group converges to isomers A or B. The VDE values of isomers A and B are predicted to be 1.61 and 1.53 eV (Table 3), respectively, which are in good accord with the experiment.

For *cis*-$PA^{2-}(CH_3OH)_2$, the lowest energy isomer is found to have two methanol molecules each solvating one $-CO_2^-$ end (Fig. 5, iso A). The next energetically low-lying isomer is the one with one $-CO_2^-$ moiety (for instance, the β site, labeled iso B) solvated by two methanol molecules, which is 20.62 kJ/mol higher in energy. The calculated VDE of the most stable isomer A (2.29 eV) is consistent with the experimental value of 2.10 eV. Isomer B might also be present in the experiments to account for the observed low binding energy threshold X' in the spectrum.

Mixed solvent *cis*-$PA^{2-}(CH_3CN)(H_2O)_n$ (n = 1 and 2) and *cis*-$PA^{2-}(CH_3OH)(H_2O)$ clusters

For the *cis*-$PA^{2-}(CH_3CN)(H_2O)$ mixed solvent cluster, two most stable structures are identified (Fig. 6, isomers A and B),

Table 3. Comparison of experimental VDE values to calculated ones and relative energies (ΔE) of the isomers for *cis*-$PA^{2-}(CH_3CN)_m$ and *cis*-$PA^{2-}(CH_3OH)_m$ (m = 1, 2) at the M06-2X/aug-cc-pVDZ level. The isomers in bold are the ones most likely exist in the experiments.

Clusters	Isomers	ΔE (kJ/mol)	VDE (eV)	
			Calc.	Exp.
cis-$PA^{2-}(CH_3CN)$	**iso A**	0.00	1.60	1.44± 0.05
	iso B	2.55	1.53	
cis-$PA^{2-}(CH_3CN)_2$	**iso A**	0.00	2.12	2.08 ± 0.05
	iso B	22.40	1.74	
cis-$PA^{2-}(CH_3OH)$	**iso A**	0.00	1.61	1.44 ± 0.05
	iso B	0.38	1.53	
cis-$PA^{2-}(CH_3OH)_2$	**iso A**	0.00	2.29	2.10 ± 0.10
	iso B	20.62	1.67	1.60 ± 0.10

in which each of the two $-CO_2^-$ ends is separately solvated by one acetonitrile and one water molecule, respectively. The next low energy isomer C is found to feature a structure in which both acetonitrile and water molecules reside on one $-CO_2^-$ end by forming two $O^-\cdots H-O$ H-bonds with H_2O, and by formation of two $O^-\cdots H-C$ (of methyl) H-bonds with CH_3CN, and one extra inter-solvent H-bond between O of H_2O and the third H of methyl group in CH_3CN. Because total five H-bonds are formed in isomer C, this structure is calculated to be quite favorable, only 7.81 kJ/mol higher in energy than the global minimum. A third solvation scenario, in which the acetonitrile molecule solvates one $-CO_2^-$ moiety by forming three $O^-\cdots H-C$ (of methyl) H-bonds, and the water molecule binds to the N terminal of CH_3CN via the formation of a single N···H(OH) bond, is also identified (iso D). However, this structure is quite high in energy, lying 51.66 kJ/mol above isomer A, and ~44 kJ/mol above isomer C. The calculated VDEs of isomers A/B (2.12/2.11 eV) and isomer C (1.74 eV) (Table 4) align well with the EBE positions of the main spectral band X, and the low binding energy band X', respectively, suggesting these isomers are all populated in the experiments. It is interesting to note that the X' band is significant, implying that the formation of H-bonded network in-between the acetonitrile and water solvents is preferred.

Adding a second water to the naked $-CO_2^-$ end of isomer C of *cis*-$PA^{2-}(CH_3CN)(H_2O)$ at the α or β site results in isomers A and B of the *cis*-$PA^{2-}(CH_3CN)(H_2O)_2$ cluster, respectively, which are predicted to be the lowest energy structures and are energetically nearly degenerate. Isomer C, in which two waters solvate one $-CO_2^-$ moiety and one acetonitrile solvates the other $-CO_2^-$, is identified and calculated to lie 11.72 kJ/mol above isomer A. A third type of isomer, in which three solvent molecules form a solvent-cage and this cage solvates only one $-CO_2^-$ group (isomer D), is also found and predicted to be 27.85 kJ/mol higher in energy than isomer A. It can be seen from

Table 4 that the calculated VDE values of three low-lying isomers A–C are 2.44, 2.35, and 2.29 eV, respectively, which

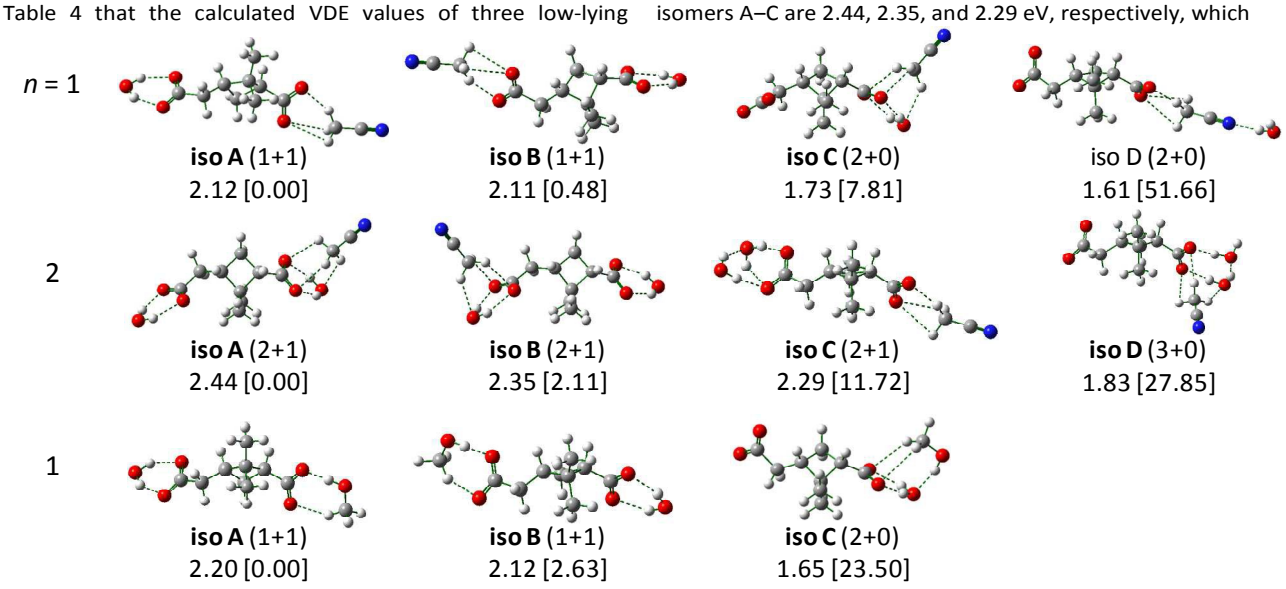

Fig. 6. M06-2X/aug-cc-pVDZ optimized structures of *cis*-PA^{2-}(SoI)$(H_2O)_n$ (SoI = CH_3CN and CH_3OH; n = 1, 2 as indicated in the first column) (O, red; C, gray; H, light gray). The calculated VDEs (in eV) and relative energies (ΔE in kJ/mol, inside square brackets) are given. The isomers in bold are the ones most likely exist in the experiments.

are all close to the experimental VDE of 2.29 eV for the main spectral feature. The calculated VDE of isomer D is 1.83 eV, consistent reasonably with the experimental VDE of 1.60 eV obtained from the minor spectral band X'.

Table 4. Comparison of experimental VDE values to calculated ones and relative energies (ΔE) of the isomers for *cis*-$PA^{2-}(CH_3CN)(H_2O)_n$ (n = 1, 2) and *cis*-$PA^{2-}(CH_3OH)(H_2O)$ at the M06-2X/aug-cc-pVDZ level. The isomers in bold are the ones most likely exist in the experiments.

Clusters	Isomers	ΔE (kJ/mol)	VDE (eV)	
			Calc.	Exp.
cis-$PA^{2-}(CH_3CN)(H_2O)$	**iso A**	0.00	2.12	2.07 ± 0.05
	iso B	0.48	2.11	
	iso C	7.81	1.73	1.50 ± 0.10
	iso D	51.66	1.61	
cis-$PA^{2-}(CH_3CN)(H_2O)_2$	**iso A**	0.00	2.44	2.29± 0.05
	iso B	2.11	2.35	
	iso C	11.72	2.29	
	iso D	27.85	1.83	1.60± 0.10
cis-$PA^{2-}(CH_3OH)(H_2O)$	**iso A**	0.00	2.20	2.08 ± 0.05
	iso B	2.63	2.12	
	iso C	23.50	1.65	

Similar to all clusters with two solvent molecules described above, the lowest-lying isomers A and B of *cis*-$PA^{2-}(CH_3OH)(H_2O)$ consist of methanol and water each solvating one $-CO_2^-$ group, respectively. The calculated VDEs of these two isomers, 2.20 and 2.12 eV, compare very well to the spectrum. The next low-lying isomer is identified to have an optimized structure, in which both methanol and water reside on the same side of $-CO_2^-$ end, forming four H-bonds with the negatively charged $-CO_2^-$ group and one extra H-bond in-between these two solvent molecules (isomer C). This structure lies 23.50 kJ/mol above isomer A, and its calculated VDE (1.65 eV) is appreciably smaller than the experimental VDE (2.08 eV). However, close examination of the experimental spectrum (Fig. 3) indicated that the calculated VDE of isomer C falls in the onset region, suggesting that this asymmetrically solvated (2+0) isomer may also exist and contribute to the spectrum, albeit with very small population. Nevertheless, the contribution is much smaller than that for *cis*-$PA^{2-}(H_2O)(CH_3CN)$. The binding energies of CH_3CN and CH_3OH with *cis*-$PA^{2-}(H_2O)$ are calculated to be 79.66 and 67.96 kJ/mol, respectively, exhibiting that the inter-solvent interactions for H_2O-CH_3CN is stronger than that for H_2O-CH_3OH in the complexes studied here, which support our experimental observation.

Discussions

Comparison of microhydration patterns between *cis*-PA^{2-} and aliphatic dicarboxylates DC_n^{2-} – observing asymmetric solvation for the former

Since *cis*-PA^{2-} is a dicarboxylate dianion, but linked by a rigid four-membered carbon ring and one methylene group (CH_2) between two $-CO_2^-$ ends instead of by flexible aliphatic chains $-(CH_2)_n-$ in DC_n^{2-} ($^-O_2C(CH_2)_nCO_2^-$), it would be interesting to compare the solvation patterns between *cis*-PA^{2-} of the current work and DC_n^{2-} that have been previously studied.[34-37] As expected, both dianions show preference of alternating solvation on the two negatively charged $-CO_2^-$ groups with solvent water, resulting in the odd-even variations in the EBE and spectral band shape with the addition of water as described above in detail. The broader and more complicated

bands for clusters with odd number of water than ones with even number of water are due to the fact that the number of solvent water interacting with two $–CO_2^-$ ends differs by one in the former case, while equals in the latter, which is significant for small hydrated clusters. This preference of solvation in a fashion as "symmetric" as possible is a direct consequence of the stronger CO_2^-–H_2O interaction than H_2O–H_2O interaction. Interestingly, by comparing the experiments and calculations, we are able to assign the small feature (X') at low EBE in the spectrum of *cis*-$PA^{2-}(H_2O)_2$ to the contributions of high energy (2+0) type isomers with both water solvating only one $–CO_2^-$ end. This asymmetric isomer has not been observed before for $DC_n^{2-}(H_2O)_2$ clusters, showing the subtle effect of the rigid four-membered ring substituting the flexible aliphatic chains. For the larger *cis*-$PA^{2-}(H_2O)_4$ cluster, we also found existence of this type of asymmetrically solvated (3+1) isomers, i.e., three water solvate one $–CO_2^-$ end and one water solvates the other $–CO_2^-$ end in the experiments; while only the (2+2) type solvated structures were exclusively found in the spectra for $DC_n^{2-}(H_2O)_4$ clusters. The observation of high energy asymmetrically solvated isomers in *cis*-$PA^{2-}(H_2O)_{2,4}$ but not in $DC_n^{2-}(H_2O)_{2,4}$ may be indicative of the barriers between symmetrically solvated clusters (global minima) and asymmetric ones (high energy) are significantly higher in *cis*-PA^{2-} than in DC_n^{2-}, as a result of the rigid four-remembered ring in backbone that links the two carboxylate ends in the former dianionic species. The isomerization barrier in-between the (1+1) and (2+0) structures for *cis*-$PA^{2-}(H_2O)_2$ is estimated to be about 67 kJ/mol. It is worth pointing out that high energy isomers in several cluster systems were found to be kinetically trapped even at low temperatures.[52-55]

Comparison of solvation patterns of *cis*-PA^{2-} in different solvents

Distinctly different interaction motifs between $–CO_2^-$ group and various solvents are unraveled in this work. Specifically, H_2O interacts with the $–CO_2^-$ group of *cis*-PA^{2-} via a bidentate $O^-\cdots H–O$ H-bond, CH_3CN interacts with *cis*-PA^{2-} through its methyl hydrogens by forming a tridentate $O^-\cdots H–C$ H-bond, and CH_3OH interacts with *cis*-PA^{2-} by forming two H-bonds via its hydroxyl hydrogen $O^-\cdots H–O$ and one of its methyl hydrogens $O^-\cdots H–C$ with the $–CO_2^-$ group. Interestingly, in the spectrum of *cis*-$PA^{2-}(CH_3OH)_2$, we observed a low EBE band (X') which is assigned to a high energy isomer with asymmetrically solvated structure (2+0). Similar (2+0) isomer is identified in the H_2O case as well. However, for *cis*-$PA^{2-}(CH_3CN)_2$, the (2+0) type isomer has higher energy and there is also no spectral evidence for its existence in the experiments. For the mixed solvent solvated *cis*-PA^{2-} clusters, we also observed distinct differences for inter-solvent interactions. Both experiment and theory support the existence of (2+0) and (3+0) type isomers for *cis*-$PA^{2-}(CH_3CN)(H_2O)$ and *cis*-$PA^{2-}(CH_3CN)(H_2O)_2$, respectively, indicating that the inter-solvent H-bond interactions between CH_3CN and H_2O are very favorable. For the *cis*-$PA^{2-}(CH_3OH)(H_2O)$ clusters, however, small contribution from the (2+0) structure cannot be ruled out. These observed differences in solvation stem from the delicate balances between solute-solvent and solvent-solvent interactions, and provide molecular level insights why proteins have different functions and structures in different solvent environments.[28-31]

Conclusions

We studied microsolvation of *cis*-pinate by H_2O, CH_3CN, and CH_3OH using NIPES and *ab initio* calculations. Both the spectral features and EBEs show an interesting odd-even effect, indicating that the solvents alternately solvate the two negative $–CO_2^-$ groups preferably. Comparison between the experiments and calculations suggests that two types of isomers, i.e., symmetric (1+1) and asymmetric (2+0), exist for both *cis*-$PA^{2-}(H_2O)_2$ and *cis*-$PA^{2-}(CH_3OH)_2$ clusters. The existence of asymmetric isomers in *cis*-PA^{2-}, but not in DC_n^{2-}, is likely due to kinetic reasons, i.e., the barriers connecting symmetric and asymmetric structures are higher in the former. For mixed H_2O/CH_3CN solvated clusters, the (2+0) and (3+0) types of high energy isomers may also be populated in the experiments as evidenced by the appearance of small low EBE features in the spectra, and supported by calculations which show good agreement between experimental and calculated VDEs based on these structures. For the *cis*-$PA^{2-}(CH_3OH)(H_2O)$ clusters, however, small contribution from the (2+0) structure cannot be ruled out. This difference shows that the formation of inter-solvent H-bond interaction in-between H_2O and CH_3CN is much more favorable than that in-between H_2O and CH_3OH, and displays the delicate balance of solute-solvent and solvent-solvent interactions at work to determine the structures of solvated clusters. This study provides molecular level description for the interactions between carboxylate and three common solvents, and may shed light on understanding the mechanism of cluster growth and formation of atmospheric organic aerosols, as well as the different functions and structures of proteins in different solvent environments.

Acknowledgements

GLH and MV were funded by the EMSL Intramural Aerosol Science Theme Funding, and XBW was supported by the U.S. Department of Energy (DOE), Office of Science, Office of Basic Energy Sciences, Division of Chemical Sciences, Geosciences and Biosciences. The experimental work was performed using EMSL, a national scientific user facility sponsored by DOE's Office of Biological and Environmental Research and located at Pacific Northwest National Laboratory, which is operated by Battelle Memorial Institute for the DOE. The theoretical work was supported by the National Natural Science Foundation of China (Grant No. 21273232) and Hundred Talents Program of Chinese Academy of Sciences and conducted on the clusters of the Center for Theoretical and Computational Chemistry at Dalian Institute of Chemical Physics.

Notes and references

1. M. P. Rissanen, T. Kurten, M. Sipila, et al., *J. Phys. Chem. A*, 2015, **119**, 4633.
2. T. Christoffersen, J. Hjorth, O. Horie, et al., *Atmos. Environ.*, 1998, **32**, 1657.
3. S. Koch, R. Winterhalter, E. Uherek, A. Kollo, P. Neeb and G. K. Moortgat, *Atmos. Environ.*, 2000, **34**, 4031.
4. M. E. Jenkin, D. E. Shallcross and J. N. Harvey, *Atmos. Environ.*, 2000, **34**, 2837.
5. R. K. Pathak, C. O. Stanier, N. M. Donahue and S. N. Pandis, *J. Geophys. Res.*, 2007, **112**, D03201.
6. A. L. Mifflin, L. Velarde, J. Ho, et al., *J. Phys. Chem. A*, 2015, **119**, 1292.
7. N. M. Donahue, I. K. Ortega, W. Chuang, et al., *Faraday Discuss.*, 2013, **165**, 91.
8. A. Guenther, C. N. Hewitt, D. Erickson, et al., *J. Geophys. Res. Atmos.*, 1995, **100**, 8873.
9. N. M. Donahue, J. H. Kroll, S. N. Pandis and A. L. Robinson, *Atmos. Chem. Phys.*, 2012, **12**, 615.
10. C. D. O'Dowd, P. Aalto, K. Hmeri, M. Kulmala and T. Hoffmann, *Nature*, 2002, **416**, 497.
11. B. Noziere, M. Kalberer, M. Claeys, et al., *Chem. Rev.*, 2015, **115**, 3919.
12. R. Zhang, A. Khalizov, L. Wang, M. Hu and W. Xu, *Chem. Rev.*, 2012, **112**, 1957.
13. A. Laskin, J. Laskin and S. A. Nizkorodov, *Chem. Rev.*, 2015, **115**, 4335.
14. I. Riipinen, T. Yli-Juuti, J. R. Pierce, T. Petäjä, D. R. Worsnop, M. Kulmala and N. M. Donahue, *Nat. Geosci.*, 2012, **5**, 453.
15. S. Schobesberger, H. Junninen, F. Bianchi, et al., *Proc. Natl. Acad. Sci., USA*, 2013, **110**, 17223.
16. M. Kulmala, J. Kontkanen, H. Junninen, et al., *Science*, 2013, **339**, 943.
17. F. Riccobono, S. Schobesberger, C. E. Scott, et al., *Science*, 2014, **344**, 717.
18. M. Ehn, J. A. Thornton, E. Kleist, et al., *Nature*, 2014, **506**, 476.
19. T. Jokinen, T. Berndt, R. Makkonen, et al., *Proc. Natl. Acad. Sci., USA*, 2015, **112**, 7123.
20. J. L. Jimenez, M. R. Canagaratna, N. M. Donahue, et al., *Science*, 2009, **326**, 1525.
21. S. Solomon, D. Qin, M. Manning, Z. Chen, M. Marquis, K. B. A. M. Tignor, H. L. Miller and (eds.), *Cambridge University Press, Cambridge, United Kingdom and New York, NY, USA*, 2007.
22. M. Hallquist, J. C. Wenger, U. Baltensperger, et al., *Atmos. Chem. Phys.*, 2009, **9**, 5155.
23. J. Elm, T. Kurten, M. Bilde and K. V. Mikkelsen, *J. Phys. Chem. A*, 2014, **118**, 7892.
24. G.-L. Hou, W. Lin, S. H. M. Deng, J. Zhang, W.-J. Zheng, F. Paesani and X.-B. Wang, *J. Phys. Chem. Lett.*, 2013, **4**, 779.
25. D. R. Cocker, S. L. Clegg, R. C. Flagan and J. H. Seinfeld, *Atmos. Environ.*, 2001, **35**, 6049.
26. M. Gielen, *Coord. Chem. Rev.*, 1996, **151**, 41.
27. C. N. R. Rao, S. Natarajan and R. Vaidhyanathan, *Angew. Chem. Int. Ed.*, 2004, **43**, 1466.
28. T. Asakura, K. Adachi and E. Schwartz, *J. Biol. Chem.*, 1978, **253**, 6423.
29. C. Mattos and D. Ringe, *Curr. Opin. Struct. Biol.* , 2001, **11**, 761.
30. C. N. Pace, S. Treviño, E. Prabhakaran and J. M. Scholtz, *Phil. Trans. R. Soc. Lond. B*, 2004, **359**, 1225.
31. M. Khabiri, B. Minofar, J. Brezovský, J. Damborský and R. Ettrich, *J. Mol. Model.*, 2013, **19**, 4701.
32. D. Bovi, A. Mezzetti, R. Vuilleumier, M. P. Gaigeot, B. Chazallon, R. Spezia and L. Guidoni, *Phys. Chem. Chem. Phys.*, 2011, **13**, 20954.
33. L.-S. Wang, C.-F. Ding, X.-B. Wang and J. B. Nicholas, *Phys. Rev. Lett.*, 1998, **81**, 2667.
34. C.-F. Ding, X.-B. Wang and L.-S. Wang, *J. Phys. Chem. A*, 1998, **102**, 8633.
35. X. Yang, Y.-J. Fu, X.-B. Wang, P. Slavíček, M. Mucha, P. Jungwirth and L.-S. Wang, *J. Am. Chem. Soc.*, 2004, **126**, 876.
36. B. Minofar, M. Mucha, P. Jungwirth, X. Yang, Y.-J. Fu, X.-B. Wang and L.-S. Wang, *J. Am. Chem. Soc.*, 2004, **126**, 11691.
37. T. Wende, M. Wanko, L. Jiang, G. Meijer, K. R. Asmis and A. Rubio, *Angew. Chem. Int. Ed.*, 2011, **50**, 3807.
38. M. Wanko, T. Wende, M. Montes Saralegui, L. Jiang, A. Rubio and K. R. Asmis, *Phys. Chem. Chem. Phys.*, 2013, **15**, 20463.
39. C. H. Dessent, J. Kim and M. A. Johnson, *Acc. Chem. Res.*, 1998, **31**, 527.
40. A. T. Shreve, M. H. Elkins and D. M. Neumark, *Chem. Sci.*, 2013, **4**, 1633.
41. X. B. Wang and L. S. Wang, *Rev. Sci. Instrum.*, 2008, **79**, 073108.
42. G. W. T. M. J. Frisch, H. B. Schlegel, Gaussian 09. Gaussian Inc.Wallingford CT, 2009.
43. X.-B. Wang and S. R. Kass, *J. Am. Chem. Soc.*, 2014, **136**, 17332.
44. S. H. Deng, G. L. Hou, X. Y. Kong, M. Valiev and X. B. Wang, *J. Phys. Chem. A*, 2014, **118**, 5256.
45. A. Rauk, D. Yu and D. A. Armstrong, *J. Am. Chem. Soc.*, 1994, **116**, 8222.
46. E. H. Kim, S. E. Bradforth, D. W. Arnold, R. B. Metz and D. M. Neumark, *J. Chem. Phys.*, 1995, **103**, 7801.
47. X.-B. Wang, H.-K. Woo, L.-S. Wang, B. Minofar and P. Jungwirth, *J. Phys. Chem. A*, 2006, **110**, 5047.
48. X.-B. Wang, J. B. Nicholas and L.-S. Wang, *J. Chem. Phys.*, 2000, **113**, 653.
49. X. P. Xing, X. B. Wang and L. S. Wang, *J. Phys. Chem. A*, 2010, **114**, 4524.
50. X.-B. Wang, X. Yang, J. B. Nicholas and L.-S. Wang, *Science*, 2001, **294**, 1322.
51. L. Jiang, S.-T. Sun, N. Heine, J.-W. Liu, T. I. Yacovitch, T. Wende, Z.-F. Liu, D. M. Neumark and K. R. Asmis, *Phys. Chem. Chem. Phys.*, 2014, **16**, 1314.
52. G. Papadopoulos, A. Svendsen, O. V. Boyarkin and T. R. Rizzo, *J. Am. Soc. Mass Spectrom.*, 2012, **23**, 1173.
53. B. Yang and M. T. Rodgers, *Phys. Chem. Chem. Phys.*, 2014, **16**, 16110.
54. D. J. Goebbert, T. Wende, L. Jiang, G. Meijer, A. Sanov and K. R. Asmis, *J. Phys. Chem. Lett.*, 2010, **1**, 2465.
55. V. Brites, A. Cimas, R. Spezia, N. Sieffert, J. M. Lisy and M. P. Gaigeot, *J. Chem. Theory Comput.*, 2015, **11**, 871.